

室外紊流對建築物自然通風之影響

朱佳仁^{1*} 吳思磊² 張祐誠²

^{1*}國立中央大學土木工程系教授

²國立中央大學土木工程系研究生

摘要

建築物內外的空氣交換可帶入室外的新鮮空氣，稀釋掉室內的空氣污染物，改善室內的空氣品質。因此必須對建築物通風與室內汙染物傳輸機制有更深入的了解。本研究採用風洞實驗的方式研究通風與多區間建築物內部汙染物傳輸之間的關係，並採用示蹤劑濃度衰減法來量測室內外空氣交換速率，並以多頻道電子壓力計量測室內外風壓的變化。實驗流況包括剪力通風與貫流通風，研究成果顯示室外紊流強度可增加雙開口建築物剪力通風的空氣交換率，剪力通風與貫流通風的無因次通風量並不會受到模型縮尺比之影響，在改變雙開口其中一個開口面積的狀況下，發現當開口面積愈大，無因次通風量線性增大，且本研究所發展的通風計算模式可供建築設計者定量評估不同開口策略對自然通風之影響。

關鍵字：建築通風，自然通風，風洞實驗，示蹤劑濃度法

Keywords: Building ventilation, Natural ventilation, Wind tunnel experiment, Tracer gas technique

1. Introduction

People in modern societies generally spend more than 90% of their time indoors [1]. Therefore, the indoor air quality (IAQ) is of great importance to the building users. Natural ventilation is one of the most commonly used methods to remove the hazardous air pollutants (HAPs), such as CO (carbon monoxide), NO_x, SO_x, and VOCs, and to improve indoor air quality [2, 3]. However, natural ventilation is dependent on external wind speed, wind direction, indoor and outdoor temperatures, size and location of building openings. Simple and accurate model to predict the ventilation rate and concentration of indoor pollutants is vital for the utilization of natural ventilation.

The most widely used method to calculate the wind-driven ventilation rate, Q , is the orifice equation:

$$Q = C_d \cdot A \cdot \sqrt{\frac{2|P_e - P_i|}{\rho}} \quad (1)$$

where A is the cross-section area of the opening; C_d is the dimensionless discharge coefficient; ρ is the density of the air; and P_e and P_i are exterior and interior pressures of the opening, respectively. The orifice equation is based on the Bernoulli's hypothesis of incompressible, inviscid flow. The discharge coefficients given in the literature are in the range of $C_d = 0.60 \sim 0.66$ for sharp-edged openings in high Reynolds number flows [4 -5].

Chu et al. [6] used wind tunnel experiments to study wind-driven ventilation for buildings with two openings on the same external wall. Their experimental results demonstrated that when the wind direction was 0° (openings on the windward façade) and $67.5^\circ \sim 180^\circ$ (openings were on the lateral and leeward façades), the time-averaged pressure difference across the openings was insignificant and the fluctuating pressure dominated the air exchange across the openings. In addition, the exchange rate of shear-induced ventilation (wind direction is $\theta = 90^\circ$) was proportional to the external wind speed and opening area, but independent of the opening location. The exchange rate for buildings with an internal partition is lower than that without a partition when the wind direction is $\theta = 0^\circ \sim 90^\circ$.

2. Experimental setup

The experiments were carried out in an open-circuit, blowing-type wind tunnel with a test section of 1.5 m in length and 1.2 m in width. Two different cubic building models with the size of 0.22 m and 0.40 m, made of acrylic, were used for the experiments. The model was mounted on the centerline of the test section, and the distance from the entrance of the test section to the building model was 0.2 m. The schematic diagram and photograph of the experimental setup are shown in Figure 1.

The surfaces of the model were made of the smooth acrylic plate (thickness 10 mm). For the 22 cm cubic model, the external opening areas are $A_1 = A_2 = 2 \text{ cm} \times 2 \text{ cm}$ (wall porosity $r_1 = r_2 = 0.826\%$). The wind direction is defined as the incidence angle of the approaching flow to the building façade with openings.

The experiment was to study the concentration and ventilation for partitioned building with two openings on the external walls of the model. The space inside the model was separated equally into two zones by an acrylic plate (thickness 10 mm). For the 22 cm cubic model, the interior volume of each zone was 3800 cm^3 . The width of the internal opening was $w = 5 \text{ cm}$, and the height is adjustable. The internal opening area was set as $A_i = 100 \text{ cm}^2$, 25 cm^2 , 10 cm^2 , 5 cm^2 , internal opening ratio $r_i = A_i/A_w = 25\%$, 6.25% , 2.5% , 1.25% .

There were three sampling tubes inside the building model (see Figure 1). The sampling tubes were connected to an air-pump, and passed to a gas chromatography (TurboGC-800, China Chromatography Inc.). The measuring range of the gas chromatography (GC) was 1 ppm to 10,000 ppm, with a resolution of 5 ppm. The gas pumping rate was $q = 100 \text{ c.c./min}$. The ratio of the gas pumping rate q to the flow rate $q/Q = 0.33\%$ for high ventilation rates, and $q/Q = 0.86\%$ for low ventilation rates.

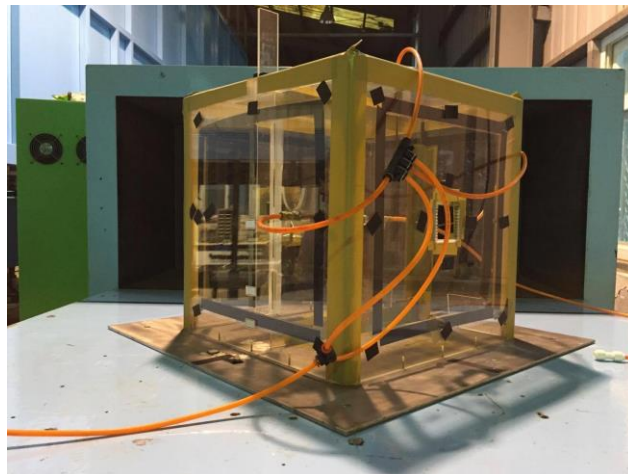
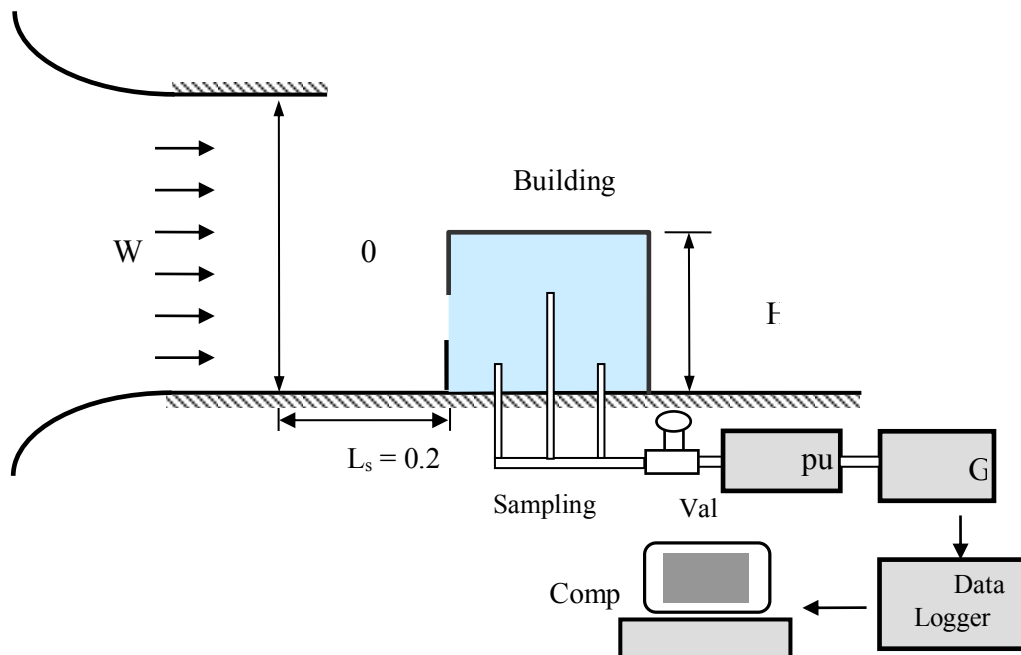


Figure 1. Schematic diagram and photograph of building model and tracer gas method.

The injection temperature of GC was set at 50°C and oven temperature of GC was 150°C. It took about 15 minutes for the temperature inside the oven to reach a constant value. At the beginning of the experiment, all of the openings on the model were sealed. The tracer gas was injected into the model for 1 minute. After the above procedures, the mixing fan was turned off and the wind tunnel and data logger (Agilent, Model: 34970A) were turned on. After the wind speed in the wind tunnel became steady, the covers on the openings were removed and the sampling procedure was started. The resolution of data logger was 15 μV , and the sampling frequency of data logger was 100 Hz. The sampling procedure took about 20 - 50 min, depending on the ventilation rate.

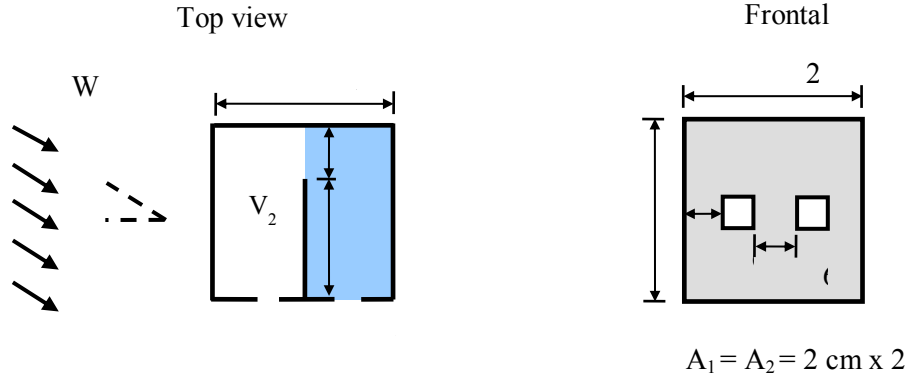


Figure 2. Schematic diagram of single-sided ventilation with internal partition.

3. Results and Discussion

3.1 Influence of model size

This part compares the measured ventilation rate of single-sided shear ventilation with two openings for 22 cm and 40 cm cubic models. For 22 cm cubic model, the wind direction was $\theta = 90^\circ$, the wall porosity $r = 0.826\%$, ($A_1 = A_2 = 2 \text{ cm} \times 2 \text{ cm}$) and the internal opening area $A_i = 100 \text{ cm}^2$ (20 cm x 5 cm). Figure 3(a) shows the relationship between the external wind speed U_H and the exchange rate of single-sided ventilation with internal partition under different wind speeds ($U = 2.32 \sim 8.6 \text{ m s}^{-1}$). The dimensionless exchange rate is defined as:

$$Q^* = \frac{Q}{U_H A_1} \quad (2)$$

As can be seen in Figure 3(b), the average dimensionless exchange rate $Q^* = 0.0488$ of present study with 22 cm model with partition is close to the experimental results $Q^* = 0.0482$ of Chu et al. [7] for the 40 cm model when wind direction $\theta = 90^\circ$. This indicates that the influence of model size (22 and 40 cm cubic models) on the dimensionless exchange rate Q^* of shear ventilation is insignificant.

3.2 Influence of opening size

This section investigates the influence of opening size on the exchange rate of shear ventilation. This experiment used the 40 cm x 40 cm x 40 cm cubic model. In this study, the opening areas were different $A_1 \neq A_2$. The area $A_1 = 4 \text{ cm} \times 4 \text{ cm}$ (wall porosity $r_1 = A_1/A_w = 1.0\%$) was fixed, and opening area A_2 has three different sizes: $A_2 = 6 \text{ cm} \times 6 \text{ cm}$, $4 \text{ cm} \times 4 \text{ cm}$, $2 \text{ cm} \times 2 \text{ cm}$, $1 \text{ cm} \times 1 \text{ cm}$ ($r_2 = A_2/A_w = 2.25\%$, 1.0% , 0.25% , 0.0625%). The external wind speed $U_H = 3.56 \text{ m/s}$, and wind direction $\theta = 90^\circ$. The internal opening area $A_i = 136.64 \text{ cm}^2$ (39.04 cm x 3.5 cm). Figure 4 shows the time histories of concentration decay for single-sided ventilation without partition, with partition, and the two-side ventilation with internal partition of different opening areas.

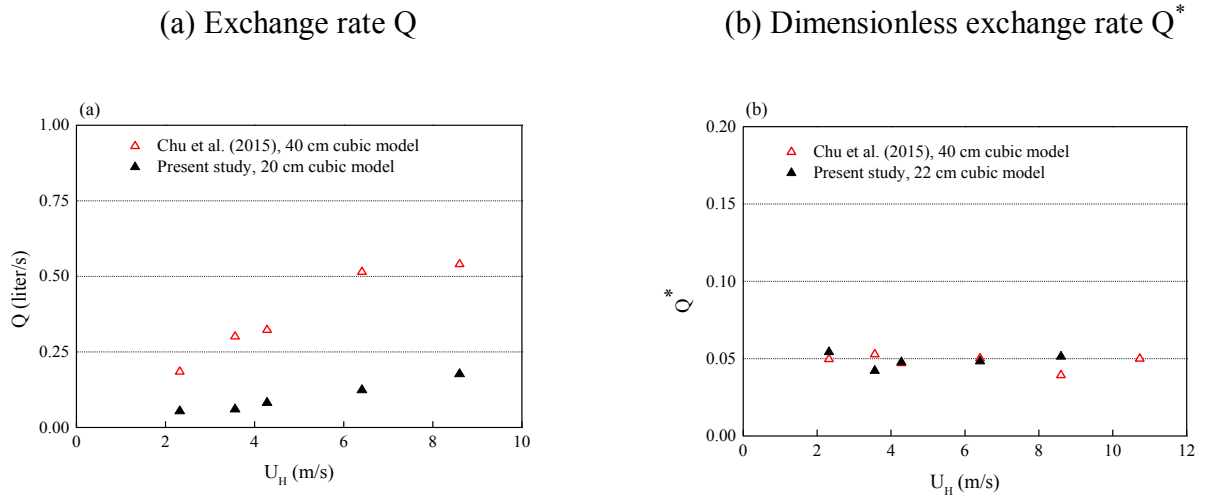


Figure 3. Relationship between the external wind speed U_H and dimensionless exchange rate Q^* of partitioned building with two openings on the same lateral wall. The wind direction $\theta = 90^\circ$, and external wall porosity $r_1 = r_2 = 1.0\%$.

Figure 5(a) compares the exchange rates Q^* of the building with and without internal partition under various wall porosity r_2 . The experimental results of Chu et al. [7] for single opening ($A_1 \neq 0, A_2 = 0$): $Q^* = 0.0175$ was also plotted in the figure for comparison. For identical openings, $A_1 = A_2$, the dimensionless exchange rate $Q^* = 0.053$ with an internal partition is smaller than the exchange rate $Q^* = 0.089$ without the partition, and this is similar to the results of Chu et al. [6]. Figure 5(b) shows the relationship between the dimensionless exchange rate Q^* and the porosity r_2 for single-sided ventilation with partition, and two-sided ventilation with partition.

3.3 Influence of turbulence intensity

This study also investigates the influence of external turbulence intensity on the exchange rate of partitioned building. This experiment used the 22 cm cubic model. In this study, the opening areas were identical $A_1 = A_2 = 2 \text{ cm} \times 2 \text{ cm}$ (wall porosity $r_1 = A_1/A_w = 0.826\%$) and the internal opening area $A_i = 100 \text{ cm}^2$ (20 cm x 5 cm). The external wind speed $U_H = 2.32 \text{ m/s}$, and wind direction $\theta = 0^\circ, 22.5^\circ, 45^\circ, 67.5^\circ, 90^\circ, 180^\circ$ under different turbulence intensity $I_u = 4.5\%$ and 14% .

Figure 6 shows the time histories of concentration variation in Room 2 under different wind directions, turbulence intensity $I_u = 14\%$. The wind speed $U_H = 2.32 \text{ m/s}$, wind direction $\theta = 0^\circ, 22.5^\circ, 45^\circ, 67.5^\circ, 90^\circ, 180^\circ$ and external wall porosity $r_1 = r_2 = 0.826\%$. The concentration decay fastest when wind direction $\theta = 0^\circ$, and slowest when $\theta = 180^\circ$. Figure 7 compares the dimensionless exchange rates Q^* under different turbulence intensity $I_u = 4.5\%$ and 14% . It demonstrates that the ventilation rate Q^* under high turbulence intensity ($I_u = 14\%$) is slightly larger than that of turbulence intensity ($I_u = 4.5\%$).

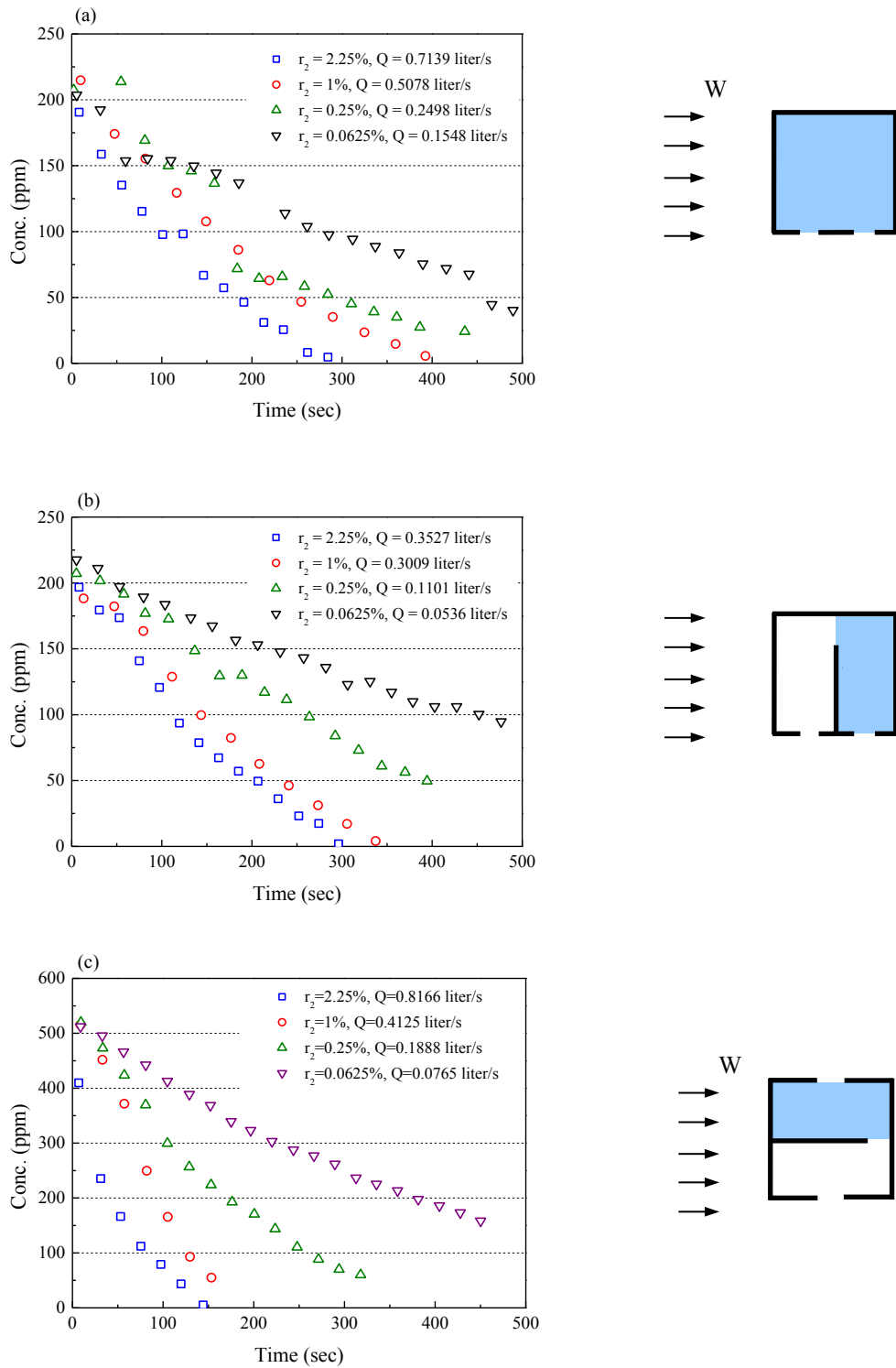


Figure 4. Time histories of concentration decay $C_1(t)$ for shear ventilation with two openings of different area on 40 cm model, wind direction = 90° . (a) Two openings on single-side; (b) Two openings on single-side with partition; (c) Two openings on two-side with partition.

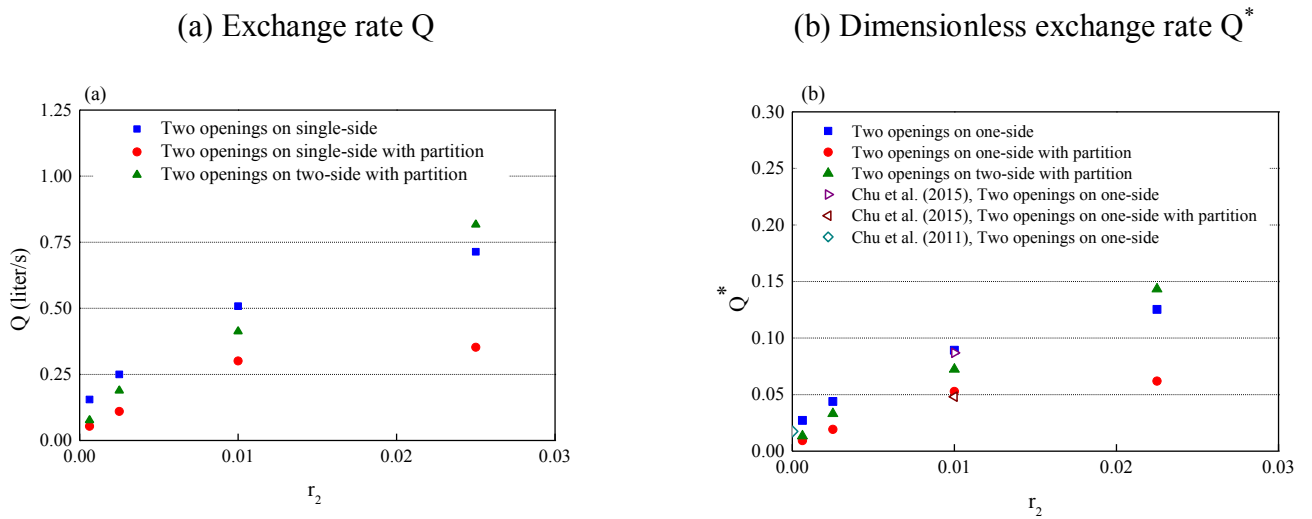


Figure 5. Relationship between the dimensionless exchange rate and wall porosity r_2 . The external wind speed $U_H = 3.56$ m/s and wind direction $\theta = 90^\circ$.

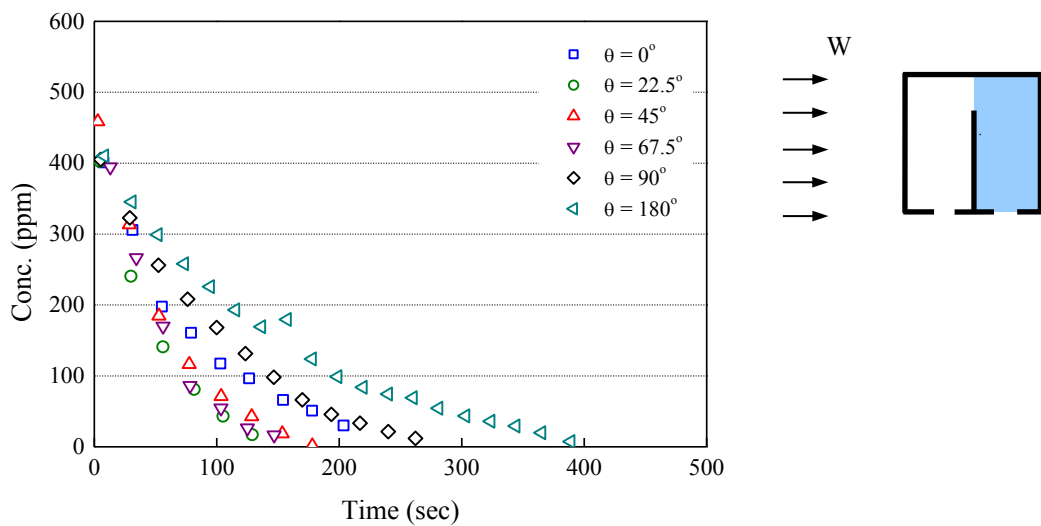


Figure 6. Time histories of concentration variation in Room 2 of different wind directions under turbulence intensity $I_u = 14\%$. The wind speed $U_H = 2.32$ m/s, wind direction $\theta = 0^\circ, 22.5^\circ, 45^\circ, 67.5^\circ, 90^\circ, 180^\circ$, and external wall porosity $r_1 = r_2 = 0.826\%$.

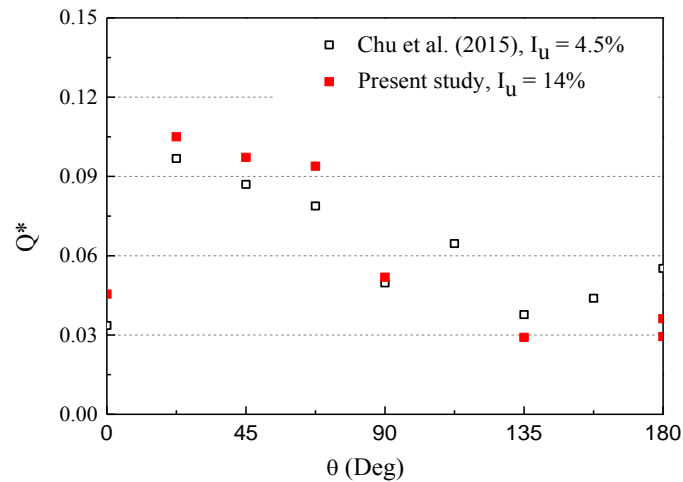


Figure 7. Comparison of the dimensionless exchange rates Q^* of two openings on the same sidewall under turbulence intensity 4.5% and 14%. The wind speed $U_H = 2.32$ and external wall porosity $r_1 = r_2 = 0.826\%$.

4. Conclusions

Natural ventilation is widely used to improve the indoor air quality and to save energy from mechanical ventilation in buildings. This study used wind tunnel experiments and tracer gas technique to investigate the wind-driven natural ventilation in a partitioned building. The experimental results indicate that the transient concentration $C(t)$ of the tracer in the building can be described by an exponential decay curve. In addition, the size of the building model has no influence on the dimensionless exchange rate Q^* . For single-sided shear ventilation, the dimensionless exchange rate Q^* increased as the area opening increased when two opening areas are different $A_1 \neq A_2$. Furthermore, the turbulence intensity of the approaching flow slightly increases the exchange rate of shear ventilation.

References

- [1] Awbi, H.B., *Ventilation of Buildings*. 2nd ed. Taylor and Francis; 2003.
- [2] Etheridge, D., Sandberg, M. *Building ventilation: Theory and measurement*, John Wiley and Sons, England; 1996.
- [3] Linden, P.F. The fluid mechanics of natural ventilation. *Annual Review of Fluid Mechanics*, 1999, 31, 201-238.
- [4] Chu, C.R., Chiu, Y.H., Chen, Y.J., Wang, Y.W., Chou, C.P. Turbulence effects on the discharge coefficient and mean flow rate of wind-driven cross ventilation. *Building and Environment*, 2009, 44, 2064-2072.
- [5] Heiselberg, P, Sandberg, M. Evaluation of discharge coefficients for window openings in wind driven natural ventilation. *International Journal of Ventilation*, 2006, 5(1), 43-52.

- [6] Chu, C.R., and Chiang, B.-F. Wind-driven cross ventilation with internal obstacles. *Energy and Buildings*, 2013, 67, 201-209.
- [7] Chu, C.R., and Wang, Y.W. The loss factors of building openings for wind-driven ventilation. *Building and Environment*, 2010, 45(10), 2273-2279.
- [8] Chu, C.R., Chiu, Y.-H. and Wang, Y.W. An experimental study of wind-driven cross ventilation in partitioned buildings. *Energy and Buildings*, 2010, 42(5), 667-673.
- [9] Chu, C.R., Chiu, Y.H., Tsai, Y.T., and Wu, S.L. Wind-driven natural ventilation for buildings with two openings on the same wall. *Energy and Buildings*, 2015, 108, 365-372.
- [10] Chu, C.R., Chen, R.H., Chen, J.W. A laboratory experiment of shear-induced ventilation. *Energy and Buildings*, 2011, 43(10), 2631-2637.